

Accretion disc evolution in single and binary T Tauri stars

P.J. Armitage¹, C.J. Clarke² and C.A. Tout^{2,3}

¹ *Canadian Institute for Theoretical Astrophysics, McLennan Labs, 60 St George Street, Toronto, Ontario M5S 3H8, Canada*

² *Institute of Astronomy, Madingley Road, Cambridge, CB3 0HA*

³ *Department of Mathematics, Monash University, Clayton, Victoria 3168, Australia*

26 March 2018

ABSTRACT

We present theoretical models for the evolution of T Tauri stars surrounded by circumstellar discs. The models include the effects of pre-main-sequence stellar and time dependent disc evolution, and incorporate the effects of stellar magnetic fields acting on the inner disc. For single stars, consistency with observations in Taurus-Auriga demands that disc dispersal occurs rapidly, on much less than the viscous timescale of the disc, at roughly the epoch when heating by stellar radiation first dominates over internal viscous dissipation. Applying the models to close binaries, we find that because the initial conditions for discs in binaries are uncertain, studies of extreme mass ratio systems are required to provide a stringent test of theoretical disc evolution models. We also note that no correlation of the infra-red colours of T Tauri stars with their rotation rate is observed, in apparent contradiction to the predictions of simple magnetospheric accretion models.

Key words: stars: pre-main-sequence – stars: magnetic fields – accretion, accretion discs – binaries: general – stars: rotation – circumstellar matter

1 INTRODUCTION

Observations of pre-main-sequence T Tauri stars suggest that stellar magnetic fields are often important in the inner regions of surrounding circumstellar discs. The field acts to provide a link between the star and its disc, and the resulting torques lead to truncation of the disc interior to some magnetospheric radius R_m (see e.g. Pringle & Rees 1972; Ghosh & Lamb 1979). This divides the accretion flow into two regimes; an outer disc where inflow is slow and the surface density of the disc material relatively large, and an inner evacuated ‘hole’ where the magnetic field is dominant and infall onto the star proceeds at approximately the free-fall velocity.

Theoretical work shows that stellar magnetic fields of the order of ~ 1 kG are a prerequisite for this mode of accretion (Königl 1991). Magnetic fields of this strength have been directly detected in a few weak-line T Tauri stars (WTTS - Basri, Marcy & Valenti 1992; Guenther & Emerson 1995, 1996), while the high X-ray flux (Montmerle 1992; Neuhäuser et al. 1995) and flaring activity (Preibisch, Zinnecker & Schmitt 1993) seen in the general T Tauri population suggest that strong magnetic fields are common. Several *consequences* of magnetospheric accretion are also observed, including mass infall at free fall velocities (Calvet & Hartmann 1992; Edwards et al. 1994; Martin 1997; Johns-Krull & Hatzes 1997), the presence of hotspots in classical T Tauri stars (CTTS - Bouvier et al. 1993), and infra-red colours

that are too red to match disc models that extend to the stellar surface (Bertout, Basri & Bouvier 1988).

Theoretical models that aim to describe the star-disc interaction are abundant (e.g. Ghosh & Lamb 1979; Campbell 1992; Yi 1994; Lynden-Bell & Boily 1994; Wang 1995, 1996; Lovelace, Romanova & Bisnovatyi-Kogan 1995; Ostriker & Shu 1995). There are important differences between these models, but a generic prediction is that the magnetospheric radius should lie close to the corotation radius (R_c , where the the disc material is stationary in the rotating stellar frame), if the magnetic linkage is to be effective in regulating the star’s angular momentum (Wang 1995; Armitage & Clarke 1996).

In recent studies, Kenyon, Yi & Hartmann (1996) and Meyer, Calvet & Hillenbrand (1997), compared the infra-red colours of a sample of classical T Tauri stars with the predictions of several steady-state magnetic and non-magnetic disc models. They concluded that the magnetically disrupted discs provided a better fit to the observed colours, and were able to place some constraints on the location of the magnetosphere relative to corotation.

In this paper, we employ time-dependent theoretical models to investigate how magnetically truncated discs evolve with time. Because the viscous timescale in the region where infrared emission originates ($R < 1$ a.u.) is small, we expect that steady-state models such as those used previously will suffice for calculating the infrared colours (assuming that the inner regions are stable). However the use of a

arXiv:astro-ph/9810490v1 30 Oct 1998

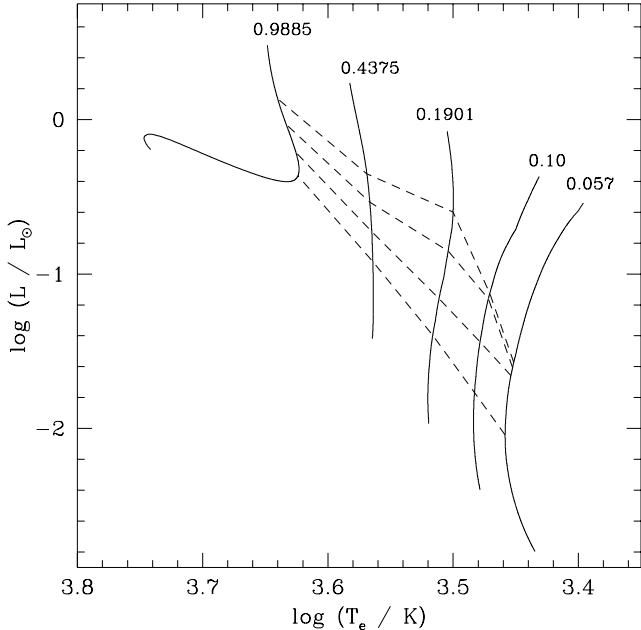


Figure 1. HR diagram for the stellar models used in this paper, with stellar masses $M_* = 0.9885, 0.4375, 0.1901, 0.10$ and $0.057 M_\odot$. Tracks are plotted started (arbitrarily) where $R_* = 3 R_\odot$, with isochrones shown relative to this time at $\Delta t = 1, 2, 4, 8$ Myr.

time-dependent approach permits us to study how rapidly the system evolves in, for example, the infrared colour-colour plane.

Section 2 describes the numerical models used in this work, which are applied in Section 3 to follow the evolution in the infra-red colour-colour diagram of discs surrounding magnetic T Tauri stars. For a limited number of systems additional information, in the form of measured stellar rotation periods, is available, and we consider the constraints this imposes in Section 4. Section 5 applies our models to discs in close binary systems. Section 6 summarises our conclusions.

2 NUMERICAL MODELLING

The numerical models employed in this work are derived from those used previously by Armitage & Clarke (1996) for modelling T Tauri systems with discs. We follow the evolution of a theoretical pre-main-sequence stellar model surrounded by a geometrically thin α -prescription (Shakura & Sunyaev 1973) accretion disc. A treatment that fully coupled the stellar evolution calculation to the disc would be essential for the early stages of accretion, here we only consider accretion rates low enough that the stellar evolution and accretion problems can be considered separately.

2.1 Stellar model

Figure 1 shows the Hertzsprung-Russell diagram for the theoretical pre-main-sequence models employed in this paper. We construct our stellar models using the most recent version of the Eggleton evolution program (Eggleton 1971,

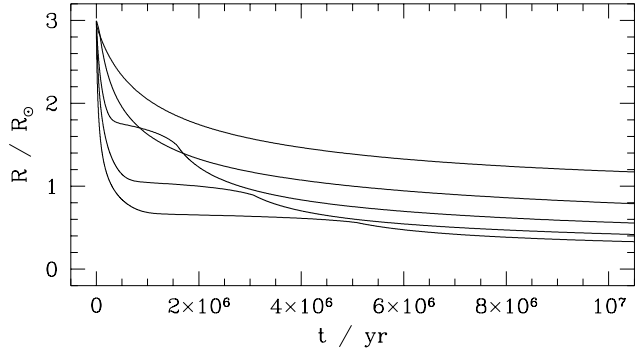


Figure 2. Time evolution of the stellar radii, for models with stellar masses (from top downwards) $M_* = 0.9885, 0.4375, 0.1901, 0.10$ and $0.057 M_\odot$.

1972, 1973). The equation of state, which includes molecular hydrogen, pressure ionization and coulomb interactions, is discussed by Pols et al. (1995). The initial composition is supposed to be uniform with a hydrogen abundance $X = 0.7$, helium $Y = 0.28$, deuterium $X_D = 3.5 \times 10^{-5}$ and metals $Z = 0.02$ with the meteoritic mixture determined by Anders and Grevesse (1989). Hydrogen burning is allowed by the pp chain and the CNO cycles. Deuterium burning is explicitly included at temperatures too low for the pp chain. Once the pp chain is active hydrogen is assumed to burn to He^4 via deuterium and He^3 in equilibrium. The burning of He^3 is not explicitly followed. Opacity tables are those calculated by Iglesias, Rogers and Wilson (1992) and Alexander and Ferguson (1994). An Eddington approximation (Woolley and Stibbs 1953) is used for the surface boundary conditions at an optical depth of $\tau = 2/3$ so that low-temperature atmospheres, in which convection extends out as far as $\tau \approx 0.01$ (Baraffe et al. 1995), are not modelled perfectly. However the effect on observable quantities (see Kroupa and Tout 1997) is not significant in this work.

The tracks in figure 1 are for four pre-main-sequence stars of masses 0.9885, 0.4375, 0.1901, 0.1 and $0.057 M_\odot$ shown from a radius of $3 R_\odot$ until they begin hydrogen burning at the main sequence. The most massive model establishes a radiative core well above the main sequence and so follows a Henyey track in its last stages of contraction. The other models remain fully convective although the $0.4375 M_\odot$ star will develop a radiative core on the main sequence. The actual starting point for all of our models was an accreting protostellar track in which material of the zero-age composition and with the surface state is accreted at a rate of $10^{-5} M_\odot \text{yr}^{-1}$. Accretion was interrupted when the various total masses were reached and the stars allowed to evolve freely with normal photospheric boundary conditions and constant total mass. All these models have relaxed from their accreting state by the time they reach $3 R_\odot$ and are by that time descending Hayashi tracks as typical pre-main-sequence stars. Figure 2 illustrates the evolution of radius with time for each of these stars. The three lower-mass objects show a plateau lasting between one and five million years. This corresponds to the delay in shrinkage while the stars burn their primordial deuterium. The duration of this plateau will depend on the actual value assumed for the pri-

mordial deuterium abundance. The two more massive stars have already burnt all their deuterium by the time they have shrunk to $3 R_{\odot}$ because their cores are correspondingly hotter.

The early accretion history of protostars has been considered by Stahler (1988), and by Hartmann, Kenyon & Cassen (1997). How the accretion influences pre-main-sequence evolution depends upon whether accretion at early times is via a magnetospheric or boundary layer mode, and on the amount of mass gained during high accretion rate outbursts. Here we are primarily interested in the later phases of accretion, for which purpose a rather arbitrary assignment of $t = 0$ suffices. We choose the time at which $R_* = 3 R_{\odot}$ because it corresponds to roughly to the upper limit on the inferred stellar radii of CTTS (Hartigan, Edwards & Ghandour 1995), and the radii used for models of stars suffering FU Orionis outbursts at higher accretion rates than those modelled here (Bell & Lin 1994).

2.2 Disc model

We consider a geometrically thin non-self-gravitating disc evolving under the influence of viscous and stellar magnetic torques. The evolution of the disc surface density distribution $\Sigma(R, t)$ is described by (e.g. Livio & Pringle 1992),

$$\frac{\partial \Sigma}{\partial t} = \frac{3}{R} \frac{\partial}{\partial R} \left[R^{1/2} \frac{\partial}{\partial R} (\nu \Sigma R^{1/2}) \right] + \frac{1}{R} \frac{\partial}{\partial R} \left[\frac{B_z B_{\phi} R^{5/2}}{\pi \sqrt{GM}} \right]. \quad (1)$$

Here ν is the kinematic viscosity, M the stellar mass, and B_z and B_{ϕ} the vertical and azimuthal components of the stellar magnetic field at the surface of the disc. We make the standard assumption that the vertical field B_z has a dipolar fall-off with radius at the magnetospheric radius (generally at several R_*), and use the expression for the azimuthal field given by Wang (1995),

$$\frac{B_{\phi}}{B_z} = \frac{\Omega(R) - \Omega_*}{\Omega(R)} \quad \Omega \geq \Omega_*$$

$$\frac{B_{\phi}}{B_z} = \frac{\Omega(R) - \Omega_*}{\Omega_*} \quad \Omega < \Omega_*, \quad (2)$$

where $\Omega(R)$ is the Keplerian velocity at radius R in the disc and Ω_* the angular velocity of the stellar surface. In protostellar discs where the Shakura-Sunyaev α parameter is probably $\ll 1$, this expression is likely to be valid if rapid reconnection in the corona limits the growth of B_{ϕ} . Different field geometries arise if $|B_{\phi}/B_z|$ is able to grow to a large value (Bardou & Heyvaerts 1996).

The kinematic viscosity is described using solutions to the vertically averaged equations for thin discs given in Faulkner, Lin & Papaloizou (1983). The analytic opacity fits used by Bell & Lin (1994) are used, so that in any one opacity regime the solution for $\nu(\alpha, R, \Sigma)$ is a power-law in surface density, radius, and α parameter. Transitions to different dominant opacities occur as the disc becomes cooler at greater radii and later times. At an accretion rate of $\dot{M} = 10^{-8} M_{\odot} \text{ yr}^{-1}$, and radii between 5 and 80 R_{\odot} , these solutions agree with the detailed vertical structure integrations presented by Bell & Lin (1994), using the same opacities, to within typically 20-30 %.

At low accretion rates, the thermal structure of the disc will be determined primarily by the heating from the central

star, rather than viscous dissipation within the disc. When the accretion rate falls low enough that this occurs, we keep $\nu(R)$ constant for the remainder of the evolution.

2.3 Spectral energy distributions

We calculate the disc spectral energy distribution assuming that each annulus in the disc radiates locally the energy input from viscous heating and reprocessing of stellar radiation. For models including a stellar magnetic field the work done on the disc material by magnetic torques is also included. The total heating of one side of the disc is then,

$$Q^+ = Q_{\nu}^+ + Q_{\text{B}}^+ + Q_{\text{p}}^+, \quad (3)$$

where the viscous term is the usual expression,

$$Q_{\nu}^+ = \frac{9}{8} \nu \Sigma \Omega^2, \quad (4)$$

and the magnetic contribution is given by

$$Q_{\text{B}}^+ = \frac{1}{2} (B_z B_{\phi})_{z=H} R^2 |\Omega - \Omega_*|. \quad (5)$$

The component Q_{p}^+ due to reprocessing of stellar radiation is computed using the standard expressions given by Kenyon & Hartmann (1987; see also Adams & Shu 1986). We assume a flat disc, a stellar spectrum given by a Planck function $B_{\nu}(T_e)$, and allow for the partial absorption when the disc starts to become optically thin.

Treating the disc as an isothermal slab, the energy loss rate per unit area through one side of the disc Q^- is,

$$Q^- = \pi B_{\nu}(T_{\text{disc}}) [1 - 2E_3(\tau_0)] \quad (6)$$

where,

$$E_3(\tau_0) = \tau_0^2 \int_{\tau_0}^{\infty} \frac{\exp^{-t} dt}{t^3}, \quad (7)$$

$\tau_0(\nu) = \kappa(\nu)\Sigma$ is the optical depth normal to the disk plane, and T_{disc} is determined by the requirement that $Q^+ = Q^-$.

The dust opacity $\kappa(\nu)$ is that used by Menšhchikov & Henning (1997) in their modelling of the source L1551 IRS 5, and incorporates a mixture of carbon and silicate components. Dust opacities vary considerably with the adopted grain model (Menšhchikov, private communication, see also figure 15 of Menšhchikov & Henning 1997), and this will modify the SED as the disc becomes optically thin. Additionally in the inner regions of the disc, where $T \gtrsim 1500$ K, the dust is destroyed and the remaining opacity, owing to molecules, is greatly reduced (Calvet, Patiño & Magris 1991; Alexander, Johnston & Rypma 1983). This is not included in our current calculations. However, at low accretion rates, when the temperature distribution in the disc is dominated by the reprocessing of stellar radiation, we expect this to be an important complication only in the innermost regions of the disc. For example, for a star of effective temperature $T_* = 4000$ K surrounded by a flat disc, the temperature falls below 1500 K within $3R_*$. In our evolutionary models the magnetosphere generally extends to at least this radius at late times, and so we do not expect large changes in our results if dust destruction was treated consistently.

For each model, we compute the spectral energy distribution (SED) for two system inclinations, a face-on disc system and one inclined at 60° . Infra-red colours are then

computed using the observed colours of main-sequence stars of given effective temperature (Kenyon & Hartmann, 1995), to which are added the contribution from the disc using the zero points in the UKIRT system (e.g. as quoted in the HST *NICMOS* reference manual).

3 COLOUR EVOLUTION OF MAGNETOSPHERIC ACCRETION MODELS

3.1 Initial conditions

The basic properties of T Tauri discs are now known observationally. Typical disc masses are $\sim 10^{-2} M_{\odot}$ (Osterloh & Beckwith 1995), typical accretion rates are $\sim 10^{-8} M_{\odot}\text{yr}^{-1}$ (Gullbring et al. 1998), and typical disc lifetimes are a few Myr (Strom 1995). We aim to set up initial conditions that are simultaneously compatible with these observations, while noting that observationally there is considerable scatter in all of these quantities. We especially caution as to the possible systematic errors in estimating ages from pre-main-sequence tracks (Tout, Livio & Bonnell 1998).

For our magnetic models we use the $M = 0.4375 M_{\odot}$ stellar model, and an initial steady-state disc with an accretion rate of $3 \times 10^{-7} M_{\odot}\text{yr}^{-1}$, at the upper end of the T Tauri accretion rate distribution. The initial disc mass is taken as $0.1 M_{*}$. With these parameters, experimentation showed that an α of 0.02 produced sensible values for the disc lifetime (in the Myr range) and initial radius (~ 30 a.u., though the disc would expand as it evolves). This value of α is also consistent with the findings of Hartmann et al. (1998), who considered the evolution of rather different self-similar disc models. These runs have a zero-torque outer boundary condition imposed at 30 a.u., and use 800 radial mesh points.

The models also require specification of the stellar magnetic field and stellar rotation period. We parameterise the stellar field as,

$$B_{*} = B_0 \left(\frac{P_{*}}{4\text{d}} \right)^{-1}, \quad (8)$$

and take B_0 between 250 G and 2 kG. For the stellar rotation rate, we assume that P_{*} varies smoothly between an initial spin period $P_i = 7$ d, and a final spin period $P_f = 3.5$ d, consistent with observations (Bouvier et al. 1995). The transition is smoothed according to,

$$P_{*} = P_f + \frac{(P_i - P_f)}{1 + (t/t_{\text{WTTS}})^2}, \quad (9)$$

where the time taken to reach a WTTS spin period, t_{WTTS} , is taken to be 3 Myr.

3.2 Results

Figures 3 and 4 shows the model tracks in the (K-L)-(K-N) colour plane, together with evolution of the colours with time. Also plotted is the observed distribution of Class II and Class III sources in Taurus-Auriga. The data are taken from the compilation of Kenyon & Hartmann (1995) and are not dereddened. The stars comprising the sample have a fairly broad distribution of ages (Kenyon & Hartmann 1995; see especially Fig. 16), with a typical age of ~ 1 Myr. A ‘gap’ in K-N between $1 < (K-N) < 2$ is clearly seen, for this sample

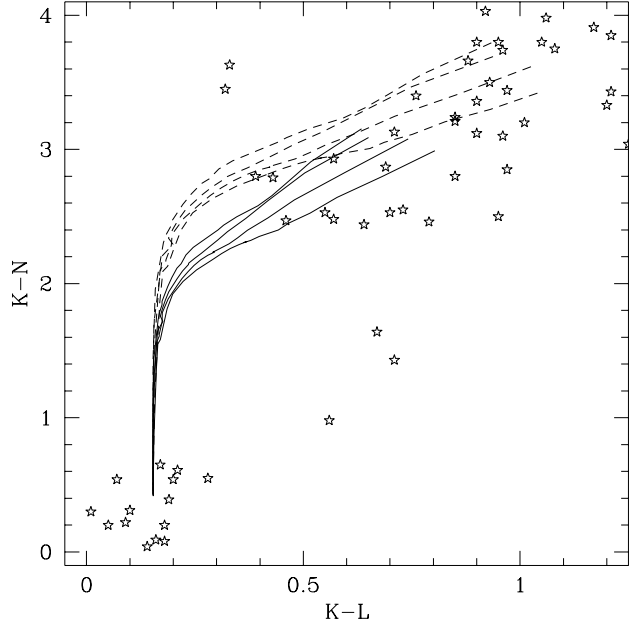


Figure 3. Tracks in the K-L, K-N plane for magnetically truncated disc models surrounding an $M_{*} = 0.4375 M_{\odot}$ star, with $B_0 = 250, 500, 1000,$ and 2000 G respectively (higher B_0 models are redder in K-N). The dashed lines are calculated for a face-on disc system, the solid lines for a disk inclined at 60° . Symbols are from the compilation of observations by Kenyon & Hartmann (1995).

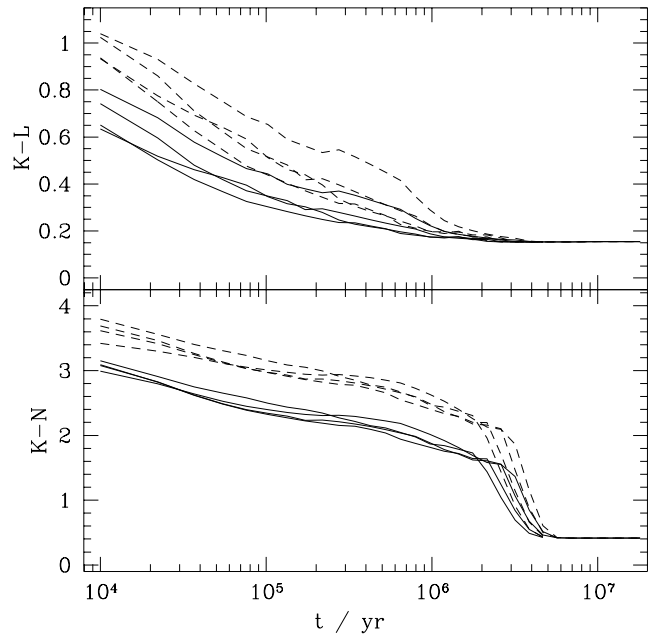


Figure 4. Time evolution of the infra-red colours corresponding to the tracks shown in Fig. 3. The dashed lines are calculated for a face-on disc system, the solid lines for a disk inclined at 60° . Note that the *absolute* time scaling is entirely determined by the assumed value of α , which is here chosen as $\alpha = 0.02$ in order to roughly match the observed lifetime of T Tauri discs.

the *only* systems lying in the gap are three binaries without separate colour information for the two components.

For a given K-L, models with stronger stellar magnetic fields are generally redder in K-N. Those models with lower B_0 , where for high accretion rates R_m is significantly smaller than R_c , seem to fit the envelope of the CTTS observations better than models with higher stellar fields, as noted previously (Kenyon, Yi & Hartmann 1996).

Our calculation of disc colours is crude – discs are probably not flat, and their spectra in the infra-red is likely to deviate substantially from a blackbody. Thus the tracks taken by the models are more significant than the absolute match with the data. Two phases of evolution occur. In the first phase, the K-L colour declines smoothly to photospheric values, while the K-N colour remains red. This first phase is driven by the decline in the accretion rate, which increases the relative importance of magnetic torques compared to the viscous torques in the inner disc, and moves the magnetosphere outward towards corotation, destroying the L flux from the disc and reducing the K-L colour. The N flux, sampling cooler parts of the disc unaffected by the magnetosphere, remains strong. This longer wavelength emission lasts until the inner disc becomes optically thin. The inclusion of the magnetic torques does not assist in producing a sharp transition between disc-like and stellar K-N colours, which instead proceeds on the slow viscous timescale of the outer disc (note that Fig. 4 is plotted on a logarithmic timescale, and thus the models predict that the amount of time spent in the unpopulated gap region is roughly equal to that spent in the allowed CTTS part of the diagram). The observation of a ‘gap’ thus unequivocally requires disc clearing to take place on a timescale much shorter than expected from purely viscous disc processes, even if stellar magnetic fields are strong enough to rapidly evacuate the inner regions of the disc out to corotation. Since mid-IR disc emission originates primarily from dust, this conclusion need not apply to the *gas* in the disc. A plausible model might envisage rapid dust agglomeration in the inner disc at the end of the CTTS phase, producing the observational effects discussed above, while the gas is dispersed on a more leisurely timescale. If this were the case, we would expect there to be systems where signatures of accretion were visible (e.g. strong H α emission), but which lacked disc emission in the infrared.

If magnetospheric accretion is commonplace, the models predict that the colours of *T Tauri* stars evolve into a region of the colour-colour plane characterised by near-photospheric K-L colour, and disc-like K-N colour. This occurs for all values of the stellar magnetic field strong enough to disrupt the inner disc at CTTS accretion rates. Strikingly, no systems are observed in this region of the diagram. Numerically, our model tracks move into this ‘empty’ region of the diagram at accretion rates of $\dot{M} \sim 10^{-8} M_\odot \text{yr}^{-1}$. This suggests either that discs are dissipated prior to stars reaching this stage (which would imply that passive reprocessing discs are likely to be rare), or that our models are missing significant extra sources of infrared flux that would shift the tracks redward into consistency with the data. The latter possibility cannot be ruled out, though if the extra flux arises from a smaller magnetosphere (for example because the magnetic coupling is weaker than assumed here), the implication would be that stellar angular momentum

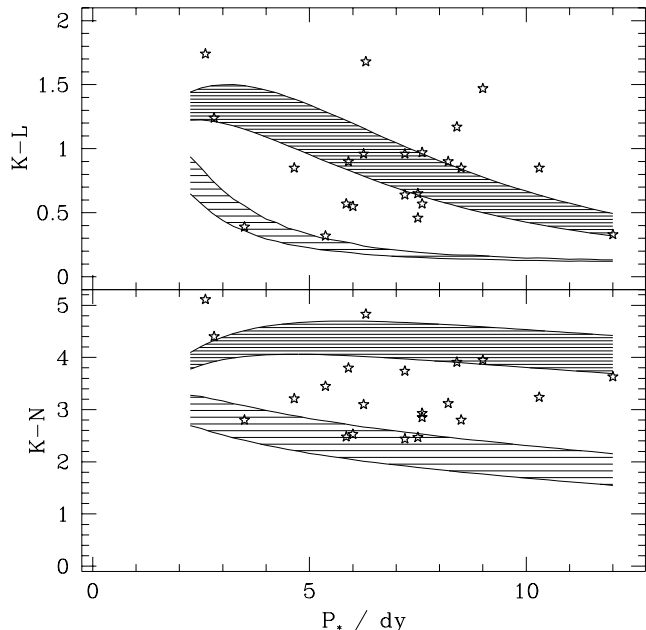


Figure 5. K-L and K-N colours (from Kenyon & Hartmann, 1995) for the CTTS with measured photometric periods P_* in the sample of Bouvier et al. (1995). The upper shaded area shows the theoretical prediction for a magnetic disc model truncated at $R_m = R_c$, with $\dot{M} = 3 \times 10^{-7} M_\odot \text{yr}^{-1}$, viewed at angles between face-on and inclined by 60° (other assumptions as stated in the text). The lower shaded area shows the predictions for a pure reprocessing disc around the same star with $\dot{M} = 0$.

regulation via magnetic coupling to the disc would be very difficult to accomplish.

Since we have already emphasized that there is considerable uncertainty in our colour calculation, we note that the same conclusion (that reprocessing dominated discs appear to be rare) follows from noting that there is no apparent pile up of systems at the lower boundary of the CTTS colour distribution, as would be expected if there were a long-lived population of discs with very low accretion rates.

4 ROTATION-COLOUR CORRELATION

In the preceding Section we considered the infra-red colour distribution of a large sample of *T Tauri* stars. For a limited subset of these, important additional information in the form of photometric periods is available. If this also represents the stellar spin period it provides a direct measure of the location of corotation, which in some models is in turn approximately equal to the magnetospheric radius. More generally, if the magnetic coupling between the star and its disc is to act to regulate the stellar angular momentum, then the rapid dipolar fall-off of $B_z(R)$ implies that R_m must lie close to R_c . This scenario then predicts that R_m should increase with increasing P_* , and lead to a correlation between the stellar spin period and the infra-red colour.

Figure 5 shows the K-L and K-N colours of the CTTS with measured photometric periods in the sample compiled by Bouvier et al. (1995). We make the standard assumption

that the photometric period traces the rotation rate of the stellar surface and plot the colours as a function of P_* . The sample comprises 22 systems, all of which have measured K-L colours in the compilation of Kenyon & Hartmann (1995), and all but one of which have measured K-N colours.

We make no pretence that this sample is in any way complete or unbiased. However the systems sampled here do cover a broad span of stellar periods, from 2 to 12 days, which represents a factor of about 3 in the implied radius of corotation. No trend in the infra-red colours is seen with varying stellar rotation period. This is obvious by eye, and a K-S test (for example) readily confirms that the K-L colours for the sample split into ‘slow’ and ‘fast’ rotators are consistent with these being drawn from a single distribution.

The Figure also shows the predictions of a steady-state version of the theoretical disc model described in Section 2 surrounding stars with varying rotation rates. We assume $R_m = R_c$, and take for the stellar parameters $M_* = M_\odot$, $R_* = 2 R_\odot$, $B_* = 1 \text{ kG}$, and $T_* = 4400 \text{ K}$. The magnetic heating term is included. The hashed area shows the range of colours expected for a disc model with an accretion rate of $3 \times 10^{-7} M_\odot \text{ yr}^{-1}$, viewed at different inclinations to the line of sight. Colours for a reprocessing disc devoid of any internal source of luminosity are also plotted.

Experimentation with the models shows that judicious variation of \dot{M} and B_* can roughly reproduce the range of colours of these CTTS (though the reddest stars with long rotation periods would demand very high accretion rates). However, if P_* is assumed to correlate well with R_m , the models all predict a strong dependence of K-L colour with rotation period. This correlation is not seen in the current data. Note that K-N colour is not expected to vary greatly with P_* , as most of the $10 \mu\text{m}$ flux comes from greater radii and is unaffected by magnetospheres of this size.

The observations display a prominent scatter that could be due to variations in accretion rate at a given rotation period or to factors not modelled in this analysis. However the dispersion, although large, would not mask the expected trend if it were uncorrelated with P_* . In particular, if we assume that the model with $\dot{M} = 3 \times 10^{-7} M_\odot \text{ yr}^{-1}$ defines the predicted theoretical trend, then the distribution of $(\text{K-L})_{\text{data}} - (\text{K-L})_{\text{model}}$ does differ significantly between slow and fast rotators. Better samples and modelling of the colours will be required to determine if this remains a problem for magnetospheric accretion models.

5 DISC EVOLUTION IN BINARY SYSTEMS

A large fraction of T Tauri stars are members of binary or multiple systems (Ghez 1996), and some of these are close enough to influence the evolution of circumstellar discs. We consider here the evolution of discs in these moderately close ($\sim 10 - 100 \text{ a.u.}$) binaries.

5.1 Truncation radii

Previous theoretical work has shown that the gravitational influence of a binary system on circumstellar material is expected to be twofold: the individual circumstellar discs will be truncated by the tidal effects of the companion star and

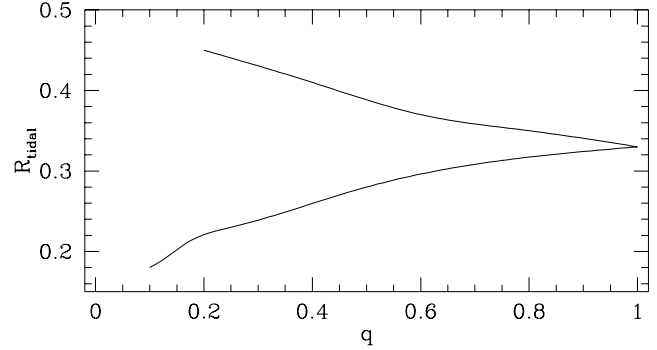


Figure 6. The assumed outer radius of the accretion disc of the primary (upper curve) and secondary (lower curve) as a fraction of the binary separation, for various mass ratios q . Adapted from Papaloizou & Pringle (1977).

a gap will be cleared between the binary and any surrounding material forming a circumbinary disc. The truncation and gap-clearing processes occur rapidly, on a dynamical timescale, and so for our purposes the initial conditions for discs in a binary can be taken as two truncated circumstellar discs. These discs will then evolve independently, *unless* a circumbinary disc exists and material is able to flow across the gap (for a review, see Lubow & Artymowicz 1996). This process is predicted to occur, though observationally circumbinary discs do not appear to be common (Mathieu 1996).

5.2 Discs in systems of varying separation

The simplest effect of binary companions on disc evolution might be expected to be a systematic variation of disc lifetime with binary separation. The reduced viscous time $t_\nu \simeq R_{\text{out}}^2 / \nu_{\text{out}}$ at the outer edge should lead to faster disc evolution in closer systems, and a higher fraction of WTTS as compared to CTTS. This effect has been searched for (Ghez, Neugebauer & Matthew 1993; Simon & Prato 1995), but although there are systems such as DI Tauri (Meyer et al. 1997) that seem to show the expected effect there appears to be no fully convincing evidence for a general trend of CTTS fraction with separation. Extension of the observations to smaller separation binaries should be able to determine if this implies ubiquitous replenishment of circumstellar discs from a circumbinary reservoir, as is already implied from the mere existence of discs in the very closest (spectroscopic) binaries.

5.3 Discs in systems with unequal mass ratios

For binaries with unequal mass ratios, we can also ask whether the different truncation radii of discs surrounding the primary and secondary will lead to observable differential disc evolution. Figure 6 shows the predicted outer radii of tidally truncated discs in a binary system as a function of the mass ratio $q = M_{\text{secondary}} / M_{\text{primary}}$ (results taken from Papaloizou & Pringle 1977; see also Paczyński 1977). We take the ‘primary’ to be the more massive star, so that $q \leq 1$. For binaries with $q \sim 0.5$, the ratio of the outer radii

Table 1. Summary of the initial conditions for the binary calculations

	M_*/M_\odot	$R_{\text{out}}/\text{a.u.}$	$\dot{M}_{\text{init}}/M_\odot \text{ yr}^{-1}$	M_{disc}/M_\odot
$q = 0.44$	0.9885	20	3×10^{-7}	0.076
	0.9885	20	3×10^{-7}	0.020
	0.4375	13.5	3×10^{-7}	0.036
	0.4375	13.5	1.3×10^{-6}	0.096
$q = 0.19$	0.9885	22.5	3×10^{-7}	0.092
	0.1901	11	3×10^{-7}	0.023
	0.1901	11	1.4×10^{-6}	0.063
$q = 0.1$	0.9885	23.5	3×10^{-7}	0.10
	0.10	9	3×10^{-7}	0.015
	0.10	9	1.4×10^{-6}	0.042

of their accretion discs is expected to be ~ 1.5 , rising to 2 – 3 for more extreme systems with $q \sim 0.1$. This disparity in radii will affect the evolutionary timescales of the two discs, while the epoch at which the transition from CTTS to WTTS status occurs will also depend on the disc initial conditions.

If the discs survive for long enough the accelerated evolution of the secondary’s smaller disc compared to the primary’s will eventually overwhelm any differences in the initial conditions of the two discs. Whatever the initial ratios of surface density, disc mass and accretion rate, at late enough epochs we thus expect that the secondary should display the weaker disc of the pair. Our numerical results aim to quantify when that switchover should occur, and how the models compare to the growing body of observations of close binary systems.

Table 1 summarises the main parameters for the numerical runs. In all cases we consider a binary with separation 50 a.u., take $\alpha = 5 \times 10^{-3}$, and impose a $v_R = 0$ boundary condition at R_{out} . The smaller value of α gives similar disc mass fractions as for the models in Section 3. 600 radial grid points are used.

The initial conditions for the primary are taken as a steady-state disc with an accretion rate of $\dot{M} = 3 \times 10^{-7} M_\odot \text{ yr}^{-1}$, that fills its Roche lobe out to R_{out} . For the $q = 0.44$ case a weakened initial disc was also run, with the same initial accretion rate but with the radial extent of the disc truncated such that M_{disc} was reduced by a factor of approximately four.

For the discs surrounding the secondaries, our standard case commences with an accretion rate equal to that of the primary. These discs are initially a factor 2-6 times less massive than the corresponding primary disc. However, cognisant of the fact that in some formation scenarios the secondary disc might accrete more infalling matter than the primary (Bate & Bonnell 1997), we also consider initially higher accretion rates through the secondary’s disc. These are chosen such that the Q parameter,

$$Q = \frac{c_s \Omega}{\pi G \Sigma} \quad (10)$$

equals unity at R_{out} , and represent the maximum plausible accretion rates through steady discs described by the vertically averaged equations. For $Q \lesssim 1$ gravitational instability sets in (Laughlin & Bodenheimer 1994), and leads to a rapid

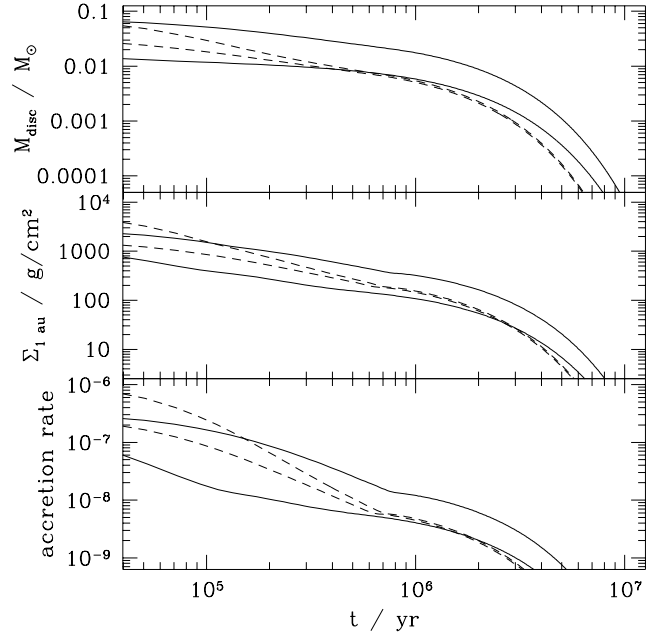


Figure 7. The decline of the disc mass, surface density at 1 a.u., and accretion rate (in $M_\odot \text{ yr}^{-1}$), for the $q = 0.44$ calculation. The solid curves show the primary disc for the standard (upper curves) and low mass (lower curve) disc initial conditions; the dashed lines show the secondary disc for high and low initial accretion rates. Here we have assumed a binary separation of 50 a.u., and taken $\alpha = 5 \times 10^{-3}$.

redistribution of disc angular momentum. A more massive disc would thus be expected to relax to a gravitationally stable configuration on a timescale that is short compared to the viscous timescales over which we compute the evolution. These high \dot{M} secondary discs have surface densities that are initially considerably higher than for the primary, and masses that are comparable, or (in the $q = 0.44$ case) slightly larger.

Figure 7 shows in detail the evolution of the discs for the runs intended to mimic a $q = 0.44$ binary system. Three possible indicators of the strength of the circumstellar discs are plotted, the total disc mass, the surface density at a radius of 1 a.u., and the accretion rate, which is expected to correlate well with measures of activity based on $H\alpha$ and UV flux.

For the standard initial conditions of the primary disc, and for all three measures of disc strength, the faster evolution of the smaller disc around the secondary is sufficient to weaken that disc below that of the primary in a relatively short time $\sim 10^6$ yr or less. The initial conditions matter most for measures based on the accretion rate, but even here the primary disc is substantially stronger than that of the secondary at accretion rates well above the typical detectable threshold.

If the disc of the primary is initially substantially smaller than the tidal truncation radius then a much longer period is required before the secondary’s disc becomes weaker than that of the primary. In particular, the accretion rate through the primary disc remains below that of the models for the secondary down to $\dot{M} \approx 3 \times 10^{-9} M_\odot \text{ yr}^{-1}$,

which would be hard to measure unambiguously observationally. Hence if the initial conditions were as biased in favour of a strong secondary disc as in this calculation they would overwhelm the faster evolution of the secondary’s disc for all observations dependent on the disc accretion rate.

5.4 Variation with mass ratio

Figure 8 summarises the results of the runs in Table 1. For each mass ratio and indicator of disc strength (disc mass, accretion rate, and surface density at an arbitrary radius of 1 a.u.) we plot the relative strength of the primary and secondary discs as a function of time. As in Section 3 we caution that the absolute time scaling of the models is somewhat arbitrary – α has been chosen so as to give plausible disc lifetimes in the Myr range.

As we have already discussed, for $q = 0.44$ the evolutionary timescales of the two discs are sufficiently similar that the initial conditions are important through to late times. For reasonable choices, there is a lengthy period when the primary and secondary discs have at least comparable strength. Observations of such binaries thus potentially retain information on the formation histories of the discs.

Few binaries appear to have very extreme mass ratios. However studies of those systems can provide a stringent test of the evolution of the disc, since for $q \lesssim 0.2 - 0.3$ the large disparity in evolutionary timescales is sufficient to rapidly overwhelm variations in the initial disc masses and radii. From Fig. 8 it can be seen that for the two most extreme mass ratios essentially all binaries are predicted to have a stronger circumprimary disc than circumsecondary. This applies for all measures of disc strength, though the disc mass is always the most robust measure.

The results can also be used to estimate the predicted fraction of ‘mixed’ systems, i.e. the number of binaries pairing a WTTS with a CTTS as a fraction of the total number of binaries containing at least one CTTS. To do this we assume that the transition from CTTS to WTTS occurs at some fixed value of the disc mass (or accretion rate or surface density) for both primary and secondary, and use the numerical models to provide the time spent as a doubly strong (CTTS + CTTS) and as a mixed (CTTS + WTTS) system.

For the $q = 0.44$ run, the results depend strongly on when the epoch of disc dispersal occurs. If the disc is lost relatively early on, when only a few viscous times have elapsed, then the predicted fraction of mixed systems depends almost entirely on the uncertain initial conditions.

For lower-mass-ratio systems, where the disparity in evolutionary timescales is greater, the influence of the initial conditions is less important. For $q = 0.19$ the time spent in the ‘mixed’ state is expected to exceed that spent as a doubly strong system, while for $q = 0.1$ the ratio of times is ~ 5 for all measures of activity (i.e. the fraction of mixed systems amongst all binaries containing at least one CTTS would be ~ 0.8). This applies even if the discs are destroyed at an accretion rate of order $10^{-8} M_{\odot} \text{yr}^{-1}$. The observation of even a few systems where the mass ratio was this extreme can thus provide a stringent test – the standard models presented here are incompatible both with a low fraction of mixed (CTTS, WTTS) systems, and with systems where the primary is weaker than the secondary at any except the

highest accretion rates. Observations to the contrary would be good evidence for accretion from a circumbinary disc.

5.5 Discussion

In this Section we have investigated the evolution of discs in close binary systems. We find that the secondary’s disc should always become weaker than that surrounding the primary at a sufficiently late epoch, but that the timing of the switchover is a strong function of the mass ratio of the binary. For mass ratios of $\gtrsim 0.5$, a secondary that has an initially higher accretion rate through its disc might remain stronger than the primary until the disc is cleared. For more extreme mass ratios, we expect the faster evolution of the smaller secondary disc to dominate over the influence of the initial conditions. At late times the secondary should display weaker disc signatures than the primary, and there should be a relatively high fraction of mixed T Tauri binaries pairing a CTTS primary with a WTTS secondary.

Current observations appear to be broadly consistent with this picture. Brandner & Zinnecker (1997) studied a sample of binaries in the 90-250 a.u. range, finding 3 systems (out of 12 containing a CTTS) where a CTTS secondary was paired with a WTTS primary. In this sample, all the measured mass ratios were $q > 0.5$, and the analysis was based on $H\alpha$ flux. This sample thus falls into the category where we would predict that the initial conditions of the discs formed around the stars should be important, and strong accretion activity among the secondaries is not unexpected.

The photometric properties of close T Tauri binaries have been studied by Prato & Simon (1997), and Ghez, White & Simon (1997). These studies show that mixed (CTTS, WTTS) binaries appear to be rare – *none* were found in the sample of 12 systems examined by Prato & Simon. This is probably marginally consistent with our models, at least if discs in these binary systems are cleared at a relatively high accretion rate. However, it is clear that a similar observational result for systems with an extreme mass ratio would be inconsistent with these independent evolution models, and would point either to common replenishment of the discs from a circumbinary disc, a much weaker dependence of t_{ν} on R than that assumed here, or a coordinated mechanism for their common destruction.

6 CONCLUSIONS

In this paper we have presented models for the evolution of circumstellar discs around T Tauri stars. The models combine a pre-main-sequence stellar evolution track with a model for viscous disc evolution. Over the estimated 1-10 Myr lifetime of T Tauri discs (Strom 1995) there are large changes in both the stellar luminosity and the disc accretion rate (Hartmann et al. 1998), making the inclusion of both components essential in an evolutionary model.

Comparison of our theoretical tracks with the distribution of infra-red colours of T Tauri stars in Taurus-Auriga (Kenyon & Hartmann 1995) yields two main conclusions. Most securely, in all models the transition in the colour-colour plane between systems looking like Classical T Tauri stars, and those appearing as Weak-lined systems, is slow,

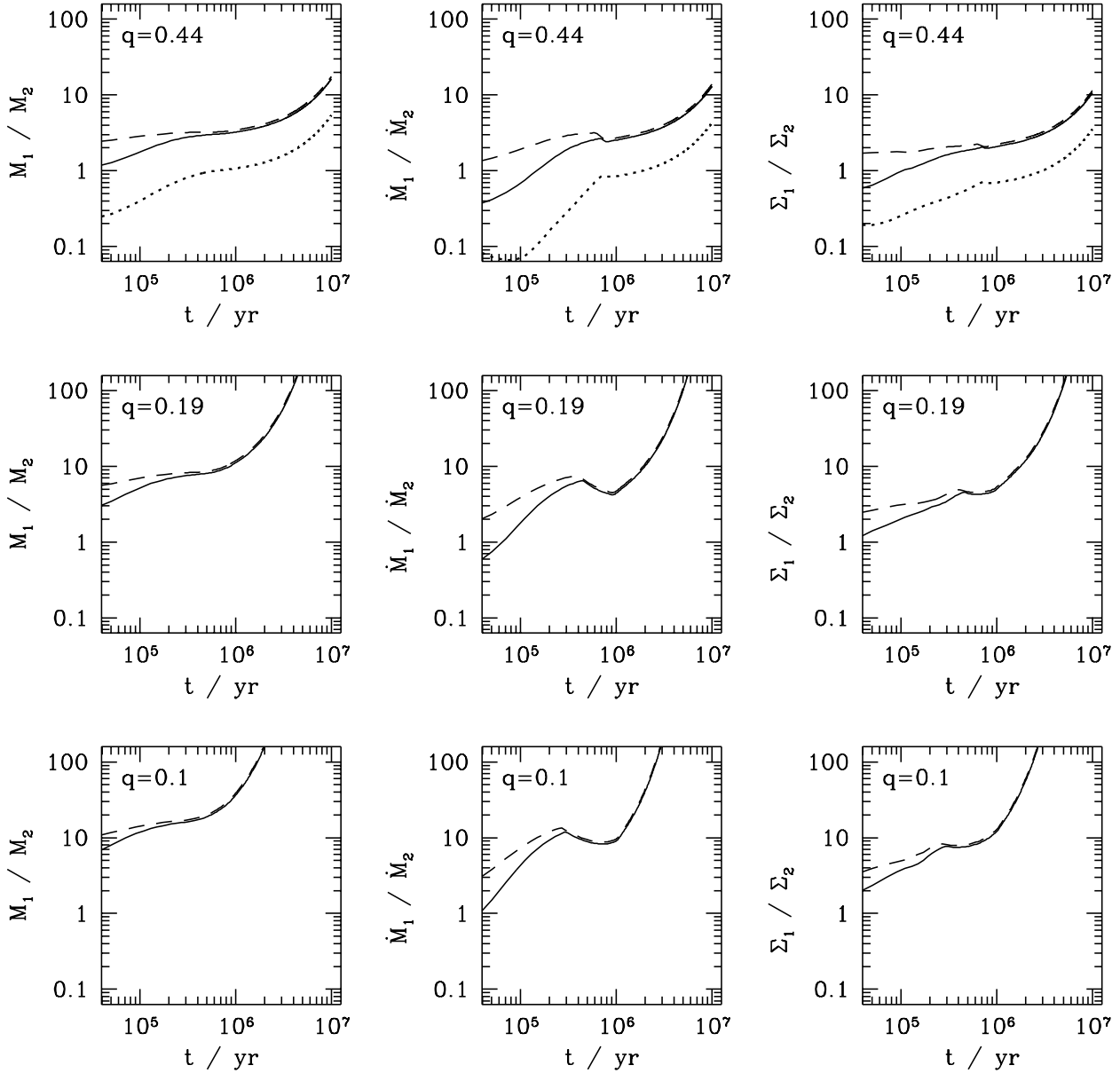


Figure 8. The relative strength of the primary and secondary discs, as a function of time, for varying mass ratios q . Disc ‘strength’ is measured by disc mass (left panels), accretion rate onto the star (centre panels), and surface density at a radius of 1 a.u. (right panels). The solid lines show the ratio of the strength of the primary to secondary discs for models where the secondary disc initially has a high accretion rate. The dashed lines show the case where the two stars have initially identical accretion rates. For a mass ratio $q = 0.44$ we also show with the dotted line the case where the primary disc is initially of low mass, as described in the text.

and occurs on the viscous timescale of the outer disc. This occurs even if a dynamically significant stellar magnetic field disrupts the inner disc. However observationally this transition *must occur very rapidly*, since there are few systems with properties intermediate between CTTS and WTTS. Non-viscous processes must be the agents of this transition.

A more detailed comparison of the models to the data provides some constraints on when disc dispersal must occur. The presence of dynamically significant stellar magnetic leads to a distinctive evolutionary track of stars in the (K-L)-(K-N) plane. As the accretion rate declines, the (K-L) colour

drops rapidly to close to bare photospheric levels while the system is still red in (K-N). No systems with this combination of colours are observed, which implies that the models can only be consistent with the observations if purely reprocessing discs are rare. We speculate that changes in the disc structure at the epoch when the disc goes from being active (heating dominated by viscous processes), to passively reprocessing stellar radiation, could be responsible for initiating the disc’s rapid demise.

Applying the models to close binary systems, we find that the observed lack of systems pairing CTTS with WTTS

is consistent with disc destruction occurring at a similar accretion rate to that inferred from the single star models. The models suggest that the frequency of mixed T Tauri binaries should increase greatly at extreme mass ratios. Observations of such systems, and studies that probe the lifetime of the CTTS phase as a function of separation, are a good indicator of T Tauri disc evolution and the ubiquity of accretion from circumbinary discs. Conversely, observations of discs in binaries with more nearly equal mass components probe the formation history of those discs, especially if observed at early epochs.

For the subsample of systems with measured photometric periods, we find no correlation between the infrared colours and the photometric period, which we assume is probably a good tracer of the stellar rotation rate. If the magnetospheric radius was approximately equal to the corotation radius, or a fixed large fraction of it, a correlation of (K-L) with P_* would be expected. The lack of such a correlation, along with suggestions that the magnetosphere lies well inside the radius of corotation (Kenyon, Yi & Hartmann 1996; Meyer, Calvet & Hillenbrand 1997), pose potentially serious problems for models that seek to explain the slow rotation of Classical T Tauri stars as a result of magnetic linkage between the star and its disc.

ACKNOWLEDGEMENTS

We thank Andrea Ghez and Scott Kenyon for very useful discussions, and Alexander Men'shchikov for supplying the dust opacity used in this work in computer readable form. The hospitality of the National Astronomical Observatory and the Isaac Newton Institute for Mathematical Sciences, where parts of this work were completed, is gratefully acknowledged.

REFERENCES

- Adams F.C., Shu F.H., 1986, *ApJ*, 308, 836
 Alexander D. R., Ferguson J.W., 1994, *ApJ*, 437, 879
 Alexander D.R., Johnson H.R., Rypma R.L., 1983, *ApJ*, 272, 773
 Anders E., Grevesse N., 1989, *Geochim. Cosmochim. Acta*, 53, 197
 Armitage P.J., Clarke C.J., 1996, *MNRAS*, 280, 458
 Baraffe I., Chabrier G., Allard F., Hauschildt P. H., 1995, *ApJ*, 446, L35
 Bardou A., Heyvaerts J., 1996, *A&A*, 307, 1009
 Basri G., Marcy G.W., Valenti J.A., 1992, *ApJ*, 390, 622
 Bate M.R., Bonnell I.A., 1997, *MNRAS*, 285, 33
 Bell K.R., Lin D.N.C., 1994, *ApJ*, 427, 987
 Bertout C., Basri G., Bouvier J., 1988, *ApJ*, 330, 350
 Bouvier J., Cabrit S., Fernández M., Martin E.L., Matthews J.M., 1993, *A&A*, 272, 176
 Bouvier J., Covino E., Kovo O., Martin E.L., Matthews J.M., Terranegra L., Beck S.C., 1995, *A&A*, 299, 89
 Brandner W., Zinnecker H., 1997, *A&A*, 321, 220
 Calvet N., Hartmann L., 1992, *ApJ*, 386, 239
 Calvet N., Patiño A., Magris G.C., 1991, *ApJ*, 380, 617
 Campbell C.G., 1992, *Geophys. Astrophys. Fluid Dyn.*, 63, 179
 Edwards S., Hartigan P., Ghandour L., Andrusis C., 1994, *AJ*, 108, 1056
 Eggleton P. P., 1971, *MNRAS*, 151, 351
 Eggleton P. P., 1972, *MNRAS*, 156, 361
 Eggleton P. P., 1973, *MNRAS*, 163, 279
 Faulkner J., Lin D.N.C., Papaloizou J., 1983, *MNRAS*, 205, 359
 Ghez A.M., 1996, in *Evolutionary Processes in Binary Stars*, eds. R.A.M.J. Wijers, M.B. Davies & C.A. Tout, Kluwer Academic Publishers, p. 1
 Ghez A.M., Neugebauer G., Matthews K., 1993, *AJ*, 106, 2005
 Ghez A.M., White R.J., Simon M., 1997, *ApJ*, 490, 353
 Ghosh P., Lamb F.K., 1979, *ApJ*, 232, 259
 Guenther E.W., Emerson J.P., 1995, in Siebenmorgen R., Käuff H.U., eds, *ESO Proceedings, The role of dust in the formation of stars*, in press
 Guenther E.W., Emerson J.P., 1996, *A&A*, 309, 777
 Gullbring E., Hartmann L., Briceno C., Calvet N., 1998, *ApJ*, 494, 323
 Hartigan P., Edwards S., Ghandour L., 1995, *ApJ*, 452, 736
 Hartmann L., Calvet N., Gullbring E., D'Alessio P., 1998, *ApJ*, 495, 385
 Hartmann L., Cassen P., Kenyon S.J., 1997, *ApJ*, 475, 770
 Iglesias C. A., Rogers F.J., Wilson B.G., 1992, *ApJ*, 397, 717
 Johns-Krull C.M., Hatzes A.P., 1997, *ApJ*, 487, 896
 Kenyon S.J., Hartmann L., 1987, *ApJ*, 323, 714
 Kenyon S.J., Hartmann L., 1995, *ApJS*, 101, 117
 Kenyon S.J., Yi I., Hartmann L., 1996, *ApJ*, 462, 439
 Königl A., 1991, *ApJ*, 370, L39
 Kroupa P., Tout C. A., 1997, *MNRAS*, 287, 402
 Laughlin G., Bodenheimer P., 1994, *ApJ*, 436, 335
 Livio M., Pringle J.E., 1992, *MNRAS*, 259, 23P
 Lovelace R.V.E., Romanova M.M., Bisnovatyi-Kogan G.S., 1995, *MNRAS*, 275, 244
 Lubow S.H., Artymowicz P., 1996, in *Evolutionary Processes in Binary Stars*, eds R.A.M.J. Wijers, M.B. Davies & C.A. Tout, Kluwer Academic Publishers, p. 53
 Lynden-Bell D., Boily C., 1994, *MNRAS*, 267, 146
 Martin S.C., 1997, *ApJ*, 478, L33
 Mathieu R.D., 1996, in *Evolutionary Processes in Binary Stars*, eds R.A.M.J. Wijers, M.B. Davies & C.A. Tout, Kluwer Academic Publishers, p. 11
 Men'shchikov A.B., Henning T., 1997, *A&A*, 318, 879
 Meyer M.R., Beckwith S.V.W., Herbst T.M., Robberto M., 1997, *ApJL*, 489, 173
 Meyer M.R., Calvet N., Hillenbrand L.A., 1997, *AJ*, 114, 288
 Montmerle T., 1992, *Mem. Soc. Astron. It.*, 63, 663
 Neuhäuser R., Sterzik M.F., Torres G., Martin E.L., 1995, *A&A*, 299, L13
 Osterloh M., Beckwith S.V.W., 1995, *ApJ*, 439, 228
 Ostriker E.C., Shu F.H., 1995, *ApJ*, 447, 813
 Paczyński B., 1977, *ApJ*, 216, 822
 Papaloizou J., Pringle J.E., 1977, *MNRAS*, 181, 441
 Pols O. R., Tout C. A., Eggleton P. P., Han Z., 1995, *MNRAS*, 274, 964
 Prato L., Simon M., 1997, *ApJ*, 474, 455
 Preibisch Th., Zinnecker H., Schmitt J.H.M.M., 1993, *A&A*, 279, L33
 Pringle J.E., Rees M.J., 1972, *A&A*, 21, 1
 Shakura N.I., Sunyaev R.A., 1973, *A&A*, 24, 337
 Simon M., Prato L., 1995, *ApJ*, 450, 824
 Stahler S.W., 1988, *ApJ*, 332, 804
 Strom S.E., 1995, *Rev. Mex. As. Ap. (Conference Series)*, 1, 317
 Tout C.A., Livio M., Bonnell I.A., 1998, *MNRAS*, in preparation
 Wang Y.-M., 1995, *ApJ*, 449, L153
 Wang Y.-M., 1996, *ApJ*, 465, L111
 Woolley R. v. d. R., Stibbs D. W. N., 1953. *The Outer Layers of a Star*. Clarendon Press, Oxford
 Yi I., 1994, *ApJ*, 428, 760